

Higher Order Statistical Analysis for Thyroid Texture Classification and Segmentation in 2D ultrasound Images

Naghmeh Mahmoodian¹, Prabal Poudel¹, Alfredo Illanes¹ and Michael Friebe¹

Abstract—Ultrasound (US) imaging is one of the most cost-effective imaging modality that utilizes sound waves for generating medical images of anatomical structure. However, the presence of speckle noise and low contrast in the US images makes it difficult to use for proper classification of anatomical structures in clinical scenarios. Hence, it is important to devise a method that is robust and accurate even in the presence of speckle noise and is not affected by the low image contrast. In this work, a novel approach for thyroid texture characterization based on extracting features utilizing higher order spectral analysis (HOSA) was used. A Support Vector Machine (SVM) was applied on the extracted features to classify the thyroid texture. Since HOSA is a well suited technique for processing non-Gaussian data involving non-linear dynamics, good classification of thyroid texture can be obtained in US images as they also contain non-Gaussian Speckle noise and non-linear characteristics. A final accuracy of 93.27%, sensitivity of 0.92 and specificity of 0.62 were obtained using the proposed approach.

I. INTRODUCTION

Thyroid is an important endocrine gland that is involved in several important body mechanisms like metabolic regulation, iodine absorption and protein synthesis. Thyroid diseases often involve changes in the shape and size of thyroid which make it essential to monitor the state as well as shape and volume of thyroid over time. We use US imaging instead of other medical image modalities as it is much safer and painless for the patients as well as easy to use with a higher availability for medical practitioners.

Several approaches have been proposed to classify and segment thyroid texture in US images [1], [2], [3]. These methods perform the segmentation by edge detection, thresholding between different gray values, region splitting and merging, active contours without edges, graph theory, segmentation based on normalized cut, localized region based active contour, distance regularized level set, fuzzy c-means algorithm, histogram clustering, QUAD tree, region and random walk.

Most of these methods are not automatic and are highly affected by the presence of speckle noise and thus require a pre-processing step. In general, it is very difficult to get rid of the speckle noise completely. In order to better deal with these noise, machine learning based approaches have been proposed, but they require a large amount of data to train the classifiers.

*This work has been funded by Federal Ministry of Education and Research in the context of the INKA Project. [Grant Number 03IPT7100X]

¹Naghmeh Mahmoodian, Prabal Poudel, Alfredo Illanes and Michael Friebe are with department of Medical Engineering, Otto-von-Guericke University, Magdeburg, Germany naghmeh.ma56@yahoo.com

HOSA method has been used for distinguishing between benign and malignant nodules in thyroid US images. These approaches involved a pre-processing step where the US images were enhanced using complex wavelet transform and finally HOSA was used to extract the features [4], [5]. However, up to our knowledge, all these approaches were used for classifying the thyroid nodules only but not the thyroid texture itself from the non-thyroid textures. Similarly, either frequency or entropy based features were used in these works to classify the thyroid nodules.

In this work, we propose a novel feature extraction technique that combines the energy, frequency and entropy based features to classify the thyroid textures. US images contain speckle noise which is known to have a non-Gaussian distribution and moreover the formation of these noise results from a non-linear process. This means that the speckle noise is dependent on the behavior of the sound propagation in the different body structure depending on the texture [6], [7]. Thus, no pre-processing has to be carried out using this approach because this method is a well suited technique for processing non-Gaussian data (i.e. the speckle noise) involving nonlinear dynamics. For that, the images are first divided into smaller texture patches and then features are extracted using HOSA, specifically bispectral analysis. The bispectral features subsequently were used for thyroid texture classification using a SVM. The results show that the features extracted from bispectrum of thyroid US image are significant to distinguish between the thyroid and non-thyroid textures in a thyroid US image. The SVM classification obtained an average test accuracy of 91.6% when a 1-fold holdout test approach was used for testing of the thyroid US images. A post-processing method was applied to improve the thyroid texture classification accuracy and produce a segmented thyroid with an accuracy of 93.27%.

II. MATERIALS AND METHODS

A. Texture Dataset Generation

We have used a publicly available dataset [8] for our work. The dataset consists of 703 thyroid US images each with an image resolution of 760×500 pixels from 6 different patients with each patient containing between 53 to 218 2D thyroid images. The images were acquired along with the ground truth manually annotated by clinical experts. The images in the dataset were divided into smaller texture patches of size 20×20 pixels to prepare a texture dataset that consisted of 667,850 texture patches in total with each image producing 950 patches. Each texture patch was labelled as either thyroid ($= 1$) or non-thyroid ($= 0$). This labelling was done by

comparing the texture patches to the ground truth obtained from expert clinicians. Fig. 1 shows an example of separation of a thyroid US images into smaller texture patches.

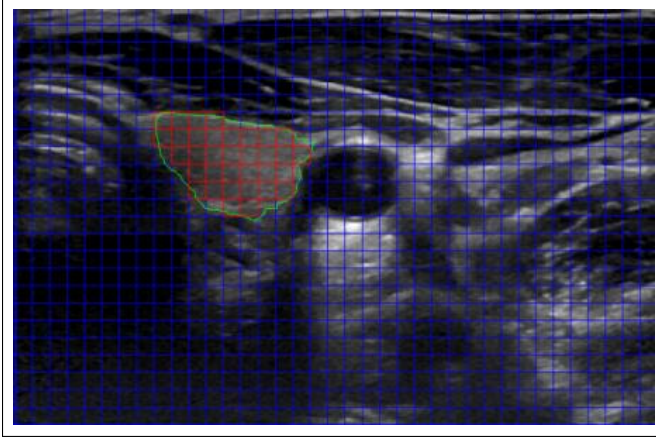


Fig. 1. Dividing of a thyroid US image into texture patches (Green: Ground-Truth, Red: Thyroid Patches, Blue: Non-Thyroid Patches)

B. Bispectral Analysis

Bispectrum is statistical analysis that falls in the category of higher order spectral which measures the spatial distribution of gray value and their deviation from its Gaussianity. One of the main advantages of bispectrum is that it allows the extraction of non-linear characteristics in an US texture patch. Additionally, it can assess the non-Gaussian property of speckle noise in US images [9].

In this work, the bispectrum is computed for each texture patch in the thyroid US images by using the Fourier Transform of a third-order cumulants sequence. In order to compute the bispectrum, first of all, the third-order moment $m_3^x(k_1, k_2)$, of $X[k]$, where $X[k]$ denotes a $N \times N$ texture patches ($N=20$) in an image and k is a 2-D index e.g., $k = [i_1, i_2]$ where $i_1, i_2 = 1, \dots, N$ and $X[k] \equiv X[i_1, i_2]$ is computed as following:

$$m_3^x(k_1, k_2) = EX(k)X(k + k_1)X(k + k_2) \quad (1)$$

where k_1 and k_2 are first and second-order correlation of $X[k]$ [10].

The third-order moment is then used to calculate the third-order cumulant of $X[k]$ using the following equation:

$$c_3^x(k_1, k_2) = m_3^x(k_1, k_2) - m_1^x[m_2^x(k_1) - m_2^x(k_2) + m_2^x(k_2 - k_1)] + 2(m_1^x)^3 \quad (2)$$

where, m_1^x corresponds to the first-order moment and m_2^x is the second-order moment.

Finally, all the three moments (i.e. first-order, second-order and third-order) are used to compute the bispectrum that is the 2-D Fourier transform of the third-order cumulant function:

$$B(f_1, f_2) = \sum_{k_1} \sum_{k_2} c_3^x(k_1, k_2) \exp^{-j(k_1 f_1 + k_2 f_2)} \quad (3)$$

where f_1 and f_2 denote discrete index spatial frequencies.

The bispectrum of Eq. 3 contains 12 symmetric regions which are repeated (redundant region), and knowing one bispectrum is sufficient to derive the others. To prevent this repetition, only $w \in \{f_1 = f_2\}$ is used for computing the bispectrum which is known as triangular region of bispectrum computation [11].

The bispectrum values were computed for each texture patches in thyroid US image. Then some features were extracted from these values for classifying the US image texture as thyroid and non-thyroid.

C. Feature extraction

The bispectrum computed using Eq. 3 is a complex matrix with large amounts of data for each texture patch. Since the computed bispectrum matrix contains large amounts of complex data, a feature extraction step is carried out to extract a set of 10 different features based on bispectral features already used in the literatures [12], [13]. A total of 10 linear and non-linear features were computed to classify thyroid and non-thyroid regions in a thyroid US image.

The linear features computed from the bispectrum are energy based and the purpose of using these features is to observe the dynamical bispectrum energy difference between thyroid and non-thyroid regions. For that we computed three different energy levels: the average, maximum and minimum computed from the bispectrum matrix of each texture patch at different locations.

The non-linear features consist of a) frequency-relation-base, that shows the dynamical difference between different frequencies in the bispectrum of thyroid and non-thyroid texture patches. These features correspond to sum of logarithmic amplitude, sum of logarithmic amplitude of diagonal elements and first-order spectral moment of amplitude of diagonal bispectrum [14]; b) entropy-based features, that compute different level of entropy in order to show the difference between regularity and irregularity properties of different texture patches. These features are entropy of phase and entropy of phase domain calculated for first, second, and third power of domain [4].

D. Classification

In this work, a SVM was used as a supervised ML approach to classify the texture in thyroid US images using the 10 features extracted using bispectrum analysis.

SVM classifier is one of the supervised classifier that perform classification class by constructing hyperplanes. SVM has the capability of data classification by using linear and non-linear kernel function. In this work, linear boundaries were used to classify an image into two linearly separable classes of thyroid and non-thyroid. A Polykernel function was used to transform feature spaces into two classes. The polykernel is defined as:

$$k(x, y) = (X^T y + c)^d \quad (4)$$

Where x and y are feature vectors from two classes and d is the degree of the polynomial. Finally, c is a regularization

parameter to control the trade-off between low error and minimizing the norm of the weight. The classification was carried out in Matlab using a 1-fold holdout testing method where 5-fold data (i.e. from 5 patients) were used for training and 1-fold data were used for testing. This process was repeated 6 times until we included each patient data in the test set.

E. Post-Processing

During classification, thyroid and non-thyroid texture patches are labeled as '1' and '0' respectively. The results of classification did not classify all the texture patches correctly. Hence, a post-processing was required after the classification step. In this regard, smoothing of the classification output vector was performed to reduce the mis-classification of the SVM. This results in a better thyroid segmentation (see Fig.2).

Each thyroid US image consists of 950 texture patches, hence 950 output labels (i.e. either 1 or 0) are produced after classification by SVM (Fig.2.a). These output labels are divided into blocks of size 6 (the block size was chosen based on the number of thyroid texture patches present in the smallest thyroid US images in the whole image dataset) resulting in a total of 158 blocks and 2 patches are left out. These two patches are considered as non-thyroid and the rest of the 158 blocks are then analyzed in two steps, firstly by counting the number of '1' in each block. The whole block is labeled as 'thyroid' if there is at least one '1' label in it and 'non-thyroid' if there is no '1' label in it (Fig.2.b). In the second step, if any block before and after the current block is labeled as thyroid, then this current block is also labeled as 'thyroid', otherwise it is labeled as non-thyroid (Fig.2.c). Finally, the outer boundary of the classified thyroid texture patches were extracted to produce a segmented thyroid as shown in the fourth row of Fig.3.

III. RESULTS AND DISCUSSIONS

The output of the bispectrum analysis is shown in Fig.4. This figure shows four different bispectrums computed from different regions in the US image. The first two bispectrum images of a1 and a2 are from non-thyroid region while b1 and b2 are from thyroid region. The observation of the computed bispectrum shows that the dynamics of texture in these two different regions are completely different from each other. We can even see this difference in the two different non-thyroid regions (i.e. in a completely black and non-black non-thyroid region), whereas the bispectra look similar in the two different thyroid regions. This is the characteristic that we want to explore to classify the texture patches in an US image as thyroid and non-thyroid.

All the 703 thyroid US images were analyzed using the proposed method. The performance of the proposed method was evaluated in the terms of accuracy, which is the number of corrected identified patches over total number of patches. The accuracy of the texture classification using SVM was 91.6% and after post-processing was 93.27%. Similarly, the Sensitivity and Specificity were 0.83 and 0.53 before

the post-processing and 0.92 and 0.62 after post-processing respectively. Fig.3 shows the classification results on four randomly selected thyroid images using SVM. These images were selected based on area the thyroid occupies in the US images (i.e. 2 left columns contain the smaller thyroid and 2 right columns contain the larger thyroid).

The results show that the proposed method can distinguish thyroid and non-thyroid texture in both the smaller and larger thyroid region (i.e. the second row in Fig.3). We also applied post-processing technique for improving the mis-classification of SVM and the results can be seen in the third row in Fig.3 and the final segmented thyroid can be seen in the fourth row in the same figure. The first row shows the ground truth binary images, which were manually annotated by the medical experts. The results show that the SVM classifier in conjunction with the post-processing step could classify the thyroid textures accurately. In the figure, the red patches represent the texture patches classified as thyroid while the green line represents the ground truth region.

The dataset was already used for thyroid segmentation by Poudel *et al.* [8]. They used classical segmentation methods such as active contour without edges (ACWE), graph cut (GC) and pixel based classifier (PBC) to segment the thyroid from the non-thyroid region. They obtained an accuracy of 73.1%, 74.8% and 67.2% using ACWE, GC and PBC respectively. Similarly, none of the approaches used in this work could segment the thyroid region in the isthmus region and on top of that ACWE even used a pre-processing step to reduce the speckle noise in the US images. These results prove that the classical segmentation approaches are not well suited for segmentation of thyroid and non-thyroid region in the US images. The approach that we have proposed in this work is the first experimental study in thyroid image texture classification and segmentation that estimates the features using HOSA. We have showed that this method can classify and segment the thyroid ultrasound images with high accuracy and do not require any pre-processing steps to reduce the speckle noise.

IV. CONCLUSION

In this work, we proposed a novel feature extraction technique using bispectrum analysis to classify and finally segment the thyroid gland in an US image using a supervised learning approach. The extracted features along with a trained classifier and a post-processing showed a good performance on thyroid texture classification. The bispectral method can even work in the presence of speckle noise as no pre-processing step was used. Similarly, since the formation of different anatomical structures in an US image is a non-linear process, bispectral analysis can easily distinguish these different structures (for example thyroid and non-thyroid structures in our case) by computing robust features for texture classification. The results show that the 10 features extracted from bispectrum computation are able to accurately classify textures in thyroid US images. In future, more research can be carried out to classify different anatomical structure in US images as well as to apply this texture

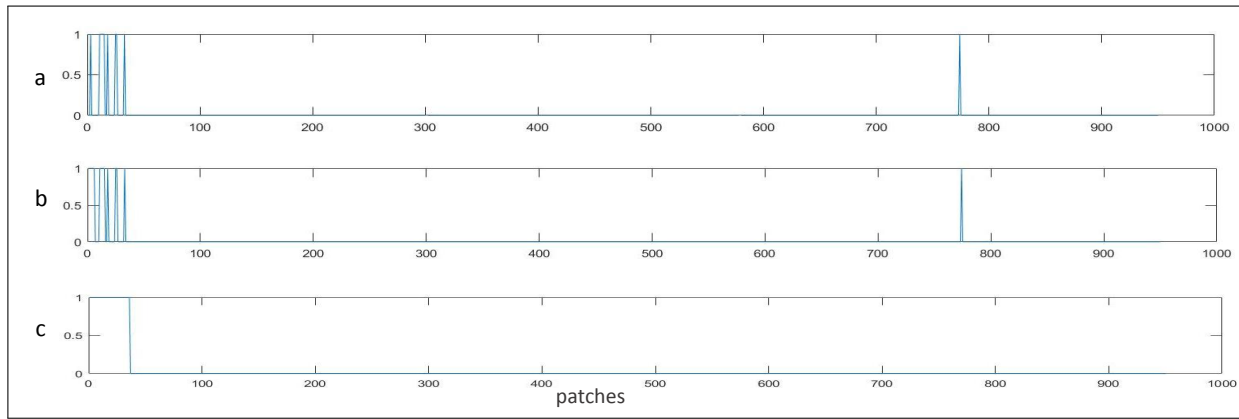


Fig. 2. An example of post-processing method for an image in dataset D01. The x and y axis are number of patches and output labels ('1' or '0') for thyroid or non-thyroid respectively. a) shows the output labels of SVM classifier, b) is the output vector of the first post-processing step and c) is the output vector of the second post-processing step.

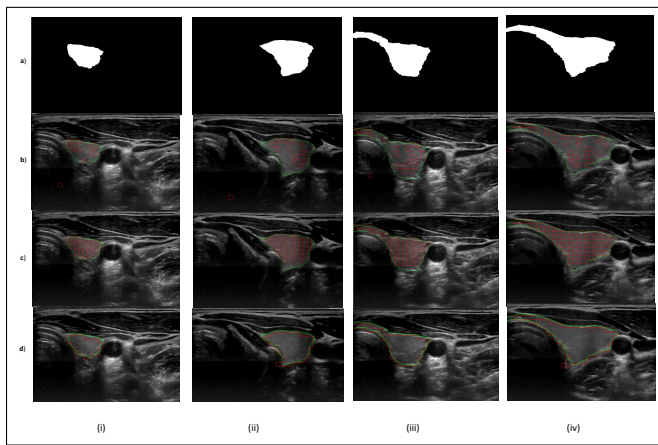


Fig. 3. Thyroid Texture Classification and Segmentation Results in 4 images of different sizes from different patients (columnwise) where a) is the ground truth, b) is the SVM classified thyroid texture patches (in red and ground truth is green), c) is thyroid texture patches after post-processing (in red) and d) is the final segmented thyroid

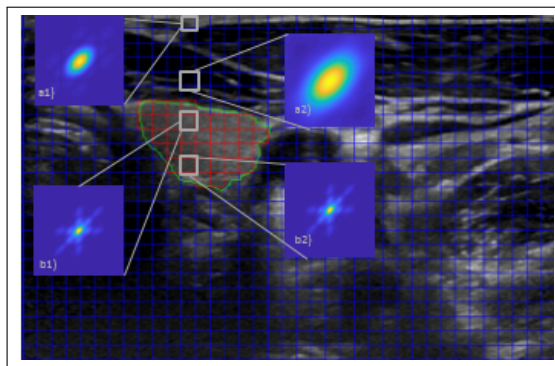


Fig. 4. Bisppectrum results of two different texture patches. a1) and a2) are the bisppectrum of non-thyroid area and b1) and b2) are the bisppectrum of the thyroid area.

classification methods on images from different imaging modality.

REFERENCES

- [1] J. Zhao, W. Zheng, L. Zhang, and H. Tian, "Segmentation of ultrasound images of thyroid nodule for assisting fine needle aspiration cytology," *Health information science and systems*, vol. 1, no. 1, pp. 5, 2013.
- [2] J. Kaur and A. Jindal, "Comparison of thyroid segmentation algorithms in ultrasound and scintigraphy images," *International Journal of Computer Applications*, vol. 50, no. 23, 2012.
- [3] A. S. Agustin, S. S. Babu and K. T. Nadu, "Thyroid segmentation on us medical images: An overview," 2012.
- [4] Acharya, U. R., Sree, S. V., Swapna, G., Gupta, S., Molinari, F., Garberoglio, R., and Suri, J. S. (2013). Effect of complex wavelet transform filter on thyroid tumor classification in three-dimensional ultrasound. *Proceedings of the Institution of Mechanical Engineers, Part H: Journal of Engineering in Medicine*, 227(3), 284-292.
- [5] Raghavendra, U., Gudigar, A., Maithri, M., Gertych, A., Meiburger, K. M., Yeong, C. H., ... and Acharya, U. R. (2018). Optimized multi-level elongated quinary patterns for the assessment of thyroid nodules in ultrasound images. *Computers in biology and medicine*, 95, 55-62.
- [6] T. E Hall and G. B. Giannakis, "Bispectral analysis and model validation of texture images," *IEEE Transactions on Image Processing*, vol. 4, no. 7, pp. 996-1009, 1995.
- [7] M. Nasrolahzadeh, Z. Mohammadpoory, and J. Haddadnia, "Higher-order spectral analysis of spontaneous speech signals in alzheimers disease," *Cognitive Neurodynamics*, pp. 1-14.
- [8] P. Poudel, A. Illanes, D. Sheet, and M. Friebe, "Evaluation of commonly used algorithms for thyroid ultrasound images segmentation and improvement using machine learning approaches," *Journal of healthcare engineering*, 2018.
- [9] A. Swami, G.B. Giannakis, and J.M. Mendel, "Linear modeling of multidimensional non-gaussian processes using cumulants," *Multidimensional Systems and Signal Processing*, vol. 1, no. 1, pp. 11-37, 1990.
- [10] M. K. Tsatsanis and G. B. Giannakis, "Object and texture classification using higher order statistics," *IEEE Transactions on Pattern Analysis and Machine Intelligence*, , no. 7, pp. 733-750, 1992.
- [11] M. E. Hossain, W. A Jassim, and M.S.A. Zilany, "Reference free assessment of speech intelligibility using bispectrum of an auditory neurogram," *PloS one*, vol. 11, no. 3, pp. e0150415, 2016.
- [12] T. Ghosh, T. Biswas, and R. Khatun, "A feature extraction scheme to classify motor imagery movements based on bi-spectrum analysis of eeg," .
- [13] D. Karimi, "Spectral and bispectral analysis of awake breathing sounds for obstructive sleep apnea diagnosis," 2013.
- [14] K.C. Chua, V. Chandran, U.R. Acharya, and C.M. Lim, "Higher order spectra based support vector machine for arrhythmia classification," in *13th International Conference on Biomedical Engineering*. Springer, 2009, pp.231-234.
- [15] R. Sharma, R.B. Pachori, and U.R. Acharya, "Application of entropy measures on intrinsic mode functions for the automated identification of focal electroencephalogram signals," *Entropy*, vol. 17, no. 2, pp. 669-691, 2015.